TECHNICAL MEMORANDUM
X-291

WIND-TUNNEL INVESTIGATION OF STATIC AERODYNAMIC CHARACTERISTICS OF A 1/9-SCALE MODEL OF A PROJECT MERCURY CAPSULE AT MACH NUMBERS FROM 1.60 TO 4.65

By David S. Shaw and Kenneth L. Turner

Langley Research Center
Langley Field, Va.

CLASSIFIED DOCUMENT - TITLE UNCLASSIFIED

NATIONAL AERONAUTICS AND SPACE ADMINISTRATION
WASHINGTON July 1960

NATIONAL AERONAUTICS AND SPACE ADMINISTRATION

TECHNICAL MEMORANDUM X-291

WIND-TUNNEL INVESTIGATION OF STATIC AERODYNAMIC CHARACTERISTICS OF A 1/9-SCALE MODEL OF A PROJECT MERCURY CAPSULE AT MACH NUMBERS FROM 1.60 TO 4.65*

By David S. Shaw and Kenneth L. Turner

SUMMARY

An investigation has been conducted in the Langley Unitary Plan wind tunnel to determine the static aerodynamic characteristics of a 1/9-scale model of a Project Mercury capsule at Mach numbers from 1.60 to 4.65. The results show that the escape configuration trims with positive stability near an angle of attack of 0° for all test Mach numbers. The pitching-moment curves near an angle of attack of 0° are nonlinear, however, and unstable characteristics are definitely shown at high angles of attack. The exit configuration trims with negative stability near an angle of attack of 0° at Mach numbers from 1.60 to 3.94. At a Mach number of 4.65, however, the capsule exhibits stable characteristics. The reentry configuration trims with positive stability near an angle of attack of 0° for all test Mach numbers.

INTRODUCTION

Numerous wind-tunnel investigations have been performed by the National Aeronautics and Space Administration on blunt, nonlifting bodies which could be used as reentry vehicles. (For example, see refs. 1 to 6.) Results of these tests have aided in the development of a reentry capsule designed to carry man into space and return. This development program has been designated "Project Mercury." The stability characteristics of this capsule must be known; consequently, wind-tunnel investigations from subsonic to hypersonic speeds over a wide range of Reynolds numbers were conducted. As a part of these tests,

*Title, Unclassified.

the Unitary Plan wind tunnel of the Langley Research Center has investigated the static aerodynamic characteristics of both the exit and reentry configurations at Mach numbers from 1.60 to 4.65, at angles of attack from -4° to 87°, and at Reynolds numbers from about 2.1×10^6 to 3.7×10^6. Included in this investigation are tests of the exit configuration with an escape system.

SYMBOLS

The aerodynamic force and moment data are referred to the body axis system (fig. 1) with the origin at the center-of-gravity locations shown in figure 2. The symbols used are defined as follows:

C_A axial-force coefficient, $\frac{\text{Axial force}}{qS}$

$C_{A_{\alpha \approx 0^{\circ}}}$ axial-force coefficient at $\alpha \approx 0^{\circ}$

$C_{A,c}$ chamber axial-force coefficient, $\frac{\text{Chamber axial force}}{qS}$

C_m pitching-moment coefficient, $\frac{\text{Pitching moment}}{qSd}$

C_{m_α} slope of pitching-moment coefficient curve at $\alpha \approx 0^{\circ}$, $\frac{\partial C_m}{\partial \alpha}$, per deg

C_N normal-force coefficient, $\frac{\text{Normal force}}{qS}$

C_{N_α} slope of normal-force coefficient curve at $\alpha \approx 0^{\circ}$, $\frac{\partial C_N}{\partial \alpha}$, per deg

d maximum body diameter, 8.278 in.

M free-stream Mach number

q free-stream dynamic pressure, lb/sq ft

R Reynolds number based on maximum diameter and free-stream conditions

S maximum cross-sectional area, 0.374 sq ft

T_t stagnation temperature, $^{\circ}F$

α angle of attack of model center line, deg

APPARATUS AND METHODS

Tunnel

Tests were conducted in both the low and the high Mach number test sections of the Langley Unitary Plan wind tunnel, which is a variable-pressure, continuous-flow tunnel. The nozzles leading to the test sections are of the asymmetric sliding-block type and permit a continuous variation in test-section Mach number from approximately 1.5 to 2.9 in the low Mach number test section and from approximately 2.3 to 4.7 in the high Mach number test section.

Model

Drawings and dimensions of the 1/9-scale test configurations are presented in figure 2. Photographs of the model are presented in figure 3. The capsule model was tested both with and without an escape system. Henceforth, the model will be referred to in terms of an escape configuration (capsule with escape system), an exit configuration (capsule with exit face forward), and a reentry configuration (capsule with reentry face forward) as noted in figure 2.

Test Conditions

Tests were performed at the following conditions:

M	R	T_t, °F	Angle-of-attack range, deg	
			Escape configuration	Exit and reentry configurations
1.60	2.7×10^6	125	-4 to 28	-4 to 87
2.06	2.5	125	-4 to 28	-4 to 87
2.87	2.4	150	-4 to 28	-4 to 87
2.87	3.7	150	-4 to 28	-4 to 87
3.94	2.9	175	-4 to 28	-4 to 87
4.65	2.1	175	-4 to 28	-4 to 87

Two separate sting arrangements were required to obtain an angle-of-attack range from -4° to 87°. Photographs of these arrangements are presented in figure 3.

The dewpoint, measured at stagnation pressure, was maintained below -30° F for all tests to assure negligible condensation effects. All tests were conducted with natural boundary-layer transition.

Measurements

Aerodynamic forces and moments were measured by means of an electrical strain-gage balance housed within the model. The balance, in turn, was rigidly fastened to a sting support system. Balance chamber pressure was measured with a single static orifice located in the balance cavity. This pressure was used to obtain the chamber axial-force coefficients. Schlieren photographs were taken at various model attitudes, Mach numbers, and Reynolds numbers. Typical schlieren photographs are presented in figures 4 to 6.

Accuracy

Based upon calibrations and repeatability of data, it is estimated that the various measured quantities are accurate within the following limits:

C_A	±0.020
$C_{A,c}$	±0.001
C_m	±0.005
C_N	±0.020
M (1.60, 2.06, 2.87, and 3.94)	±0.015
M (4.65)	±0.050
α, deg	±0.10

Corrections

Angles of attack have been corrected for both tunnel flow angularity and deflection of balance and sting system due to aerodynamic loads. The axial-force coefficients presented are for gross values. Chamber axial force, however, has been determined and is presented in figures 7 to 9.

DISCUSSION

Reynolds Number Effect

It may be seen in figures 10 to 12 that at a Mach number of 2.87 a change in Reynolds number from 2.4×10^6 to 3.7×10^6 has little or

no effect on the aerodynamic characteristics of any of the three test configurations.

Pitching Moment

The escape configuration trims with positive stability near an angle of attack of 0° throughout the test Mach number range (fig. 13) and the stability is essentially constant with Mach number. It should be noted, however, that the pitching-moment curves are nonlinear near $\alpha = 0^\circ$ and unstable characteristics are definitely shown at higher angles of attack (for example, beyond $\alpha = 12^\circ$ at $M = 1.60$). The nonlinearity of the pitching-moment curves near $\alpha = 0^\circ$ are seen to be due to the escape system when the data of figure 13 are compared with those of figure 14. Figure 14, which shows data for the exit configuration, indicates little or no nonlinearity of the pitching-moment curves near $\alpha = 0^\circ$.

The data in figure 14 show that the exit configuration trims with negative stability near an angle of attack of 0° at Mach numbers from 1.60 to 3.94. At a Mach number of 4.65, however, the capsule exhibits stable characteristics. (It is undesirable that the capsule be allowed to trim with positive stability at this attitude since the exit face has no heat shield and reentry at this attitude would be disastrous.) This same condition of trim with positive stability was noted for a similar capsule in reference 2 and this is the reason that the destabilizing device shown in figure 2(b) was incorporated into the design of the capsule. This device, however, is seen to be inadequate in producing instability.

The reentry configuration trims with positive stability near $\alpha = 0^\circ$ for all test Mach numbers as may be seen in figure 15. The break in the pitching-moment curve at an angle of attack near 15° for $M = 1.60$ at present cannot be explained; however, a similar occurrence may be noted at $M = 2.06$ for the similar capsule shape of reference 2 in this same attitude.

Normal Force

Figures 13 to 15 show that the three test configurations have positive normal-force slopes near $\alpha = 0^\circ$. The data of figure 16 show the variation of these slopes with Mach number. It is believed that the slight variations of the slopes for the reentry configuration are primarily the result of inaccuracies in measuring the small normal-force values near $\alpha = 0^\circ$.

Axial Force

The axial-force coefficients shown in figures 13 to 15, in general, exhibit the same trends with angle of attack, regardless of Mach number, for each of the three test configurations. An exception is the axial-force coefficients near $\alpha = 0^\circ$ at a Mach number of 1.60 for the reentry configuration. (See fig. 15.) For this condition the axial-force coefficients are considerably lower than expected, based on the data at the other Mach numbers. The reason for this cannot be explained with the limited data available. With this exception, the reentry configuration shows little change in axial-force coefficients near $\alpha = 0^\circ$ with Mach number in the test Mach number range. (See fig. 16.) Figure 16 also shows that the axial-force coefficients near $\alpha = 0^\circ$ for the escape and exit configurations decrease with increase in Mach number.

CONCLUSIONS

A wind-tunnel investigation has been conducted in the Langley Unitary Plan wind tunnel to determine the static aerodynamic characteristics of a 1/9-scale model of a Project Mercury capsule at Mach numbers from 1.60 to 4.65. The results of these tests indicate the following conclusions:

1. The escape configuration trims with positive stability near an angle of attack of 0° for all test Mach numbers. The pitching-moment curves near an angle of attack of 0° are nonlinear, however, and unstable characteristics are definitely shown at high angles of attack.

2. The exit configuration trims with negative stability near an angle of attack of 0° for Mach numbers from 1.60 to 3.94. At a Mach number of 4.65, however, the capsule exhibits stable characteristics.

3. The reentry configuration trims with positive stability near an angle of attack of 0° for all test Mach numbers.

Langley Research Center,
National Aeronautics and Space Administration,
Langley Field, Va., March 2, 1960.

REFERENCES

1. Turner, Kenneth L., and Shaw, David S.: Wind-Tunnel Investigation at Mach Numbers From 1.60 to 4.50 of the Static-Stability Characteristics of Two Nonlifting Vehicles Suitable for Reentry. NASA MEMO 3-2-59L, 1959.

2. Shaw, David S., and Turner, Kenneth L.: Wind-Tunnel Investigation of Static Aerodynamic Characteristics of a 1/9-Scale Model of a Possible Reentry Capsule at Mach Numbers From 2.29 to 4.65. NASA TM X-233, 1959.

3. Carter, Howard S., Kolenkiewicz, Ronald, and English, Roland D.: Principal Results From Wind-Tunnel Stability Tests of Several Proposed Space Capsule Models Up to An Angle of Attack of 33°. NASA TM X-21, 1959.

4. Pearson, Albin O.: Wind-Tunnel Investigation at Mach Numbers From 0.40 to 1.14 of the Static Aerodynamic Characteristics of a Nonlifting Vehicle Suitable for Reentry. NASA MEMO 4-13-59L, 1959.

5. Pearson, Albin O.: Wind-Tunnel Investigation at Mach Numbers From 0.20 to 1.17 of the Static Aerodynamic Characteristics of a Possible Reentry Capsule. NASA TM X-262, 1960.

6. Pearson, Albin O.: Wind-Tunnel Investigation at Mach Numbers From 0.50 to 1.14 of the Static Aerodynamic Characteristics of a Model of a Project Mercury Capsule. NASA TM X-292, 1960.

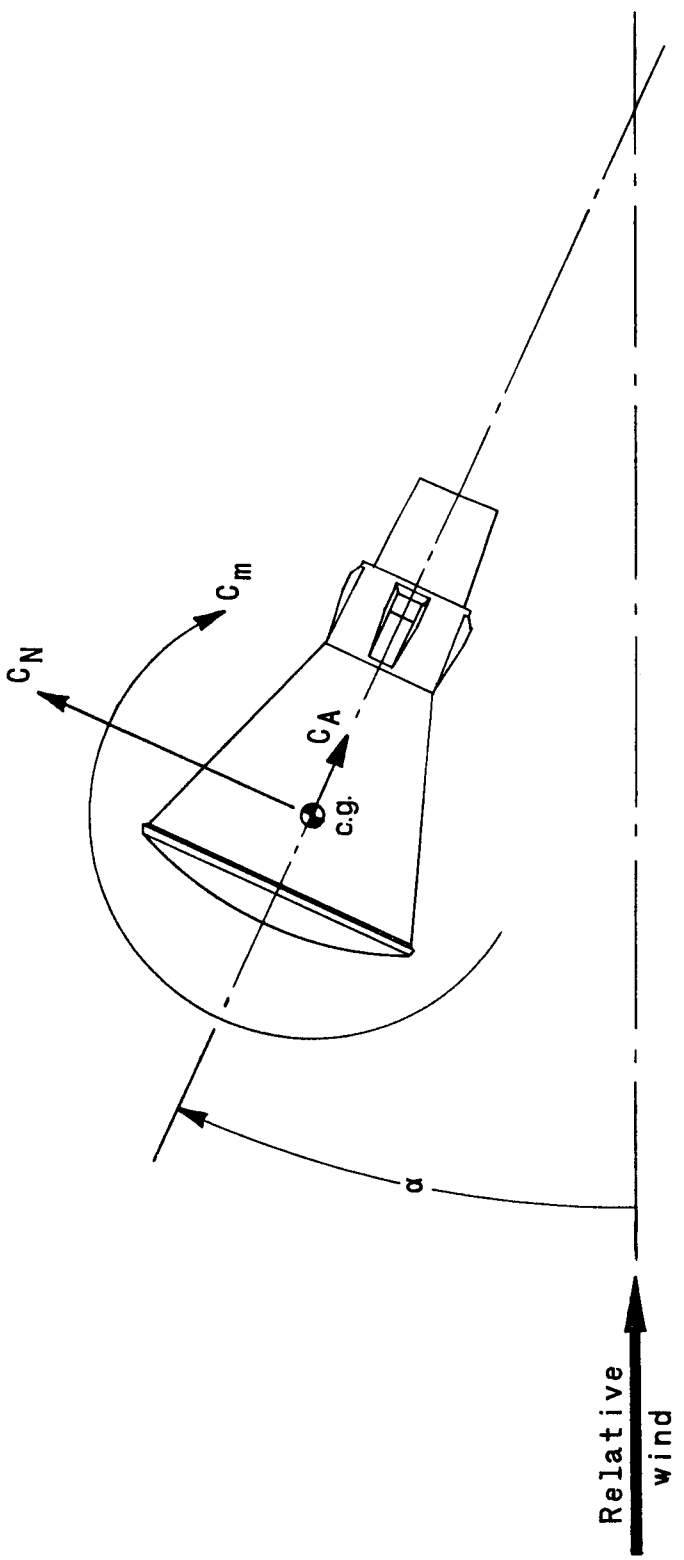

Figure 1.- Body axis system (reentry configuration shown). Arrows indicate positive direction.

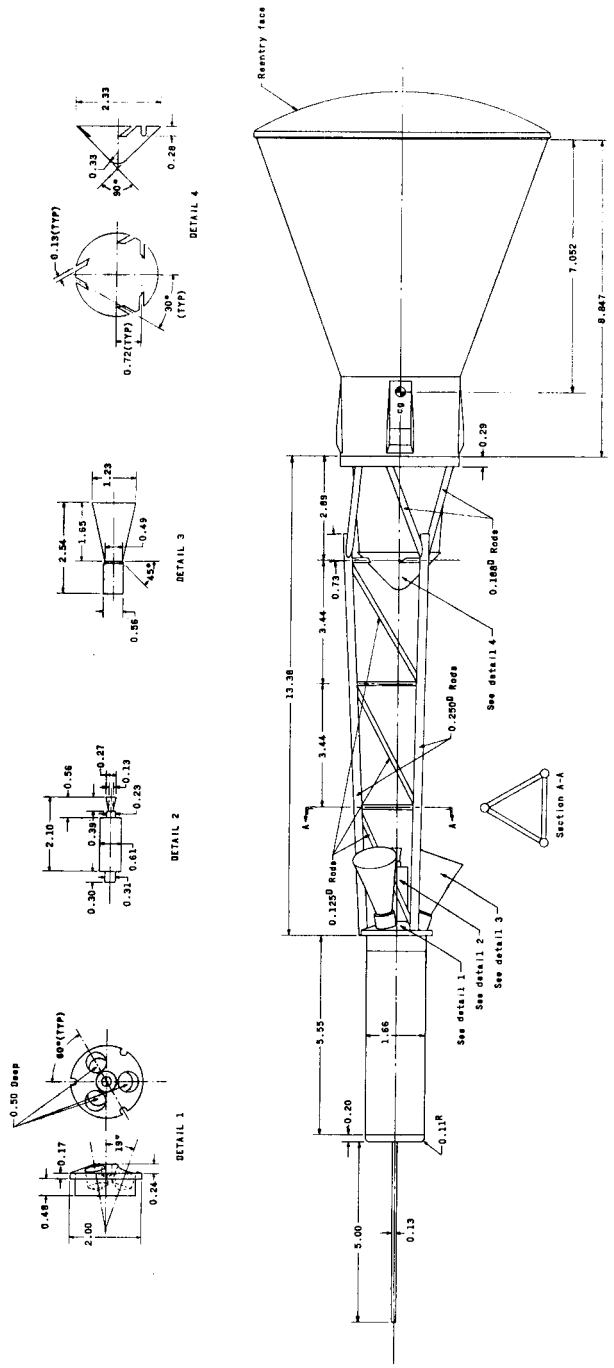

(a) Escape configuration.

Figure 2.- Drawings and dimensions of models. All dimensions are in inches unless otherwise noted.

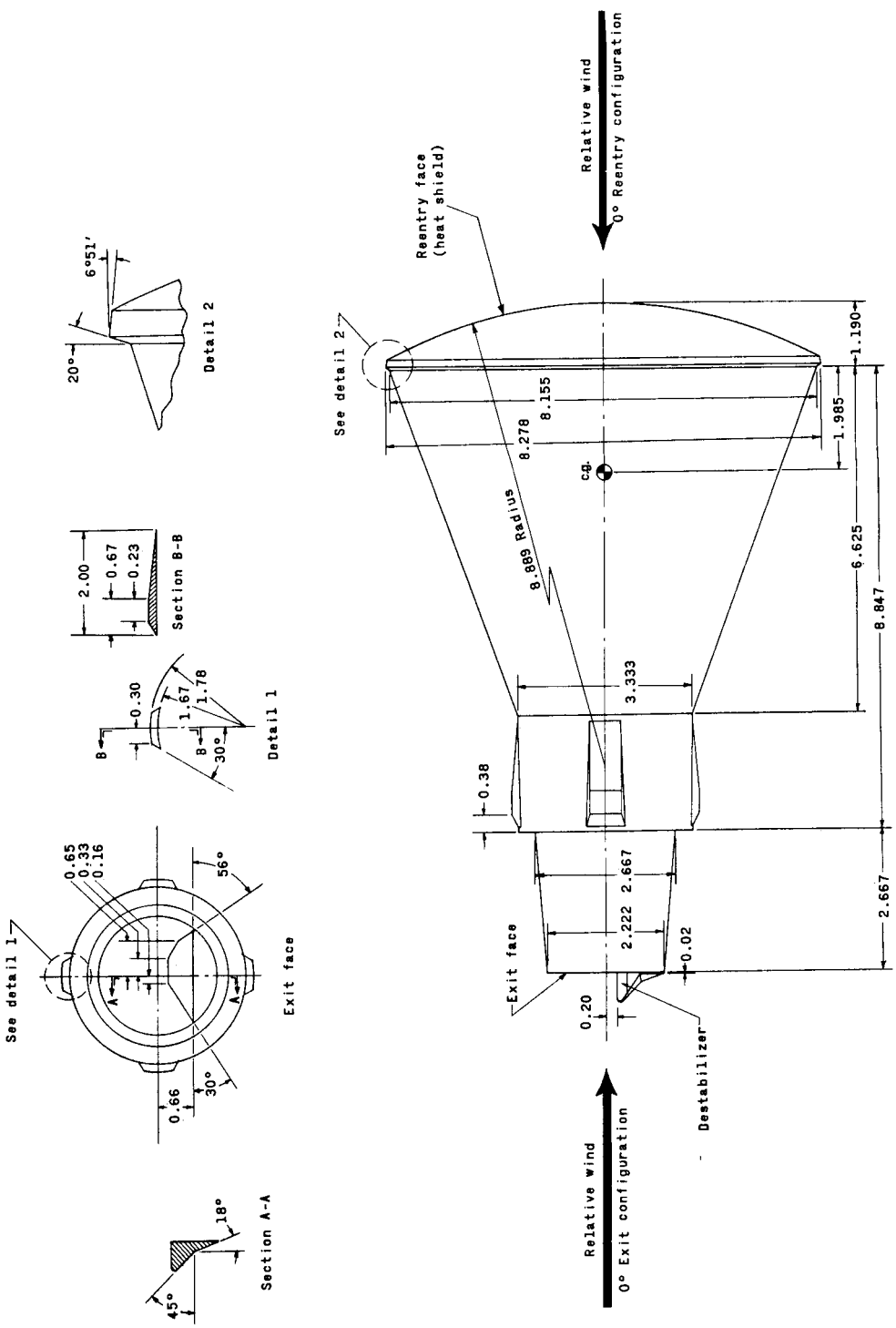

(b) Exit and reentry configuration.

Figure 2.- Concluded.

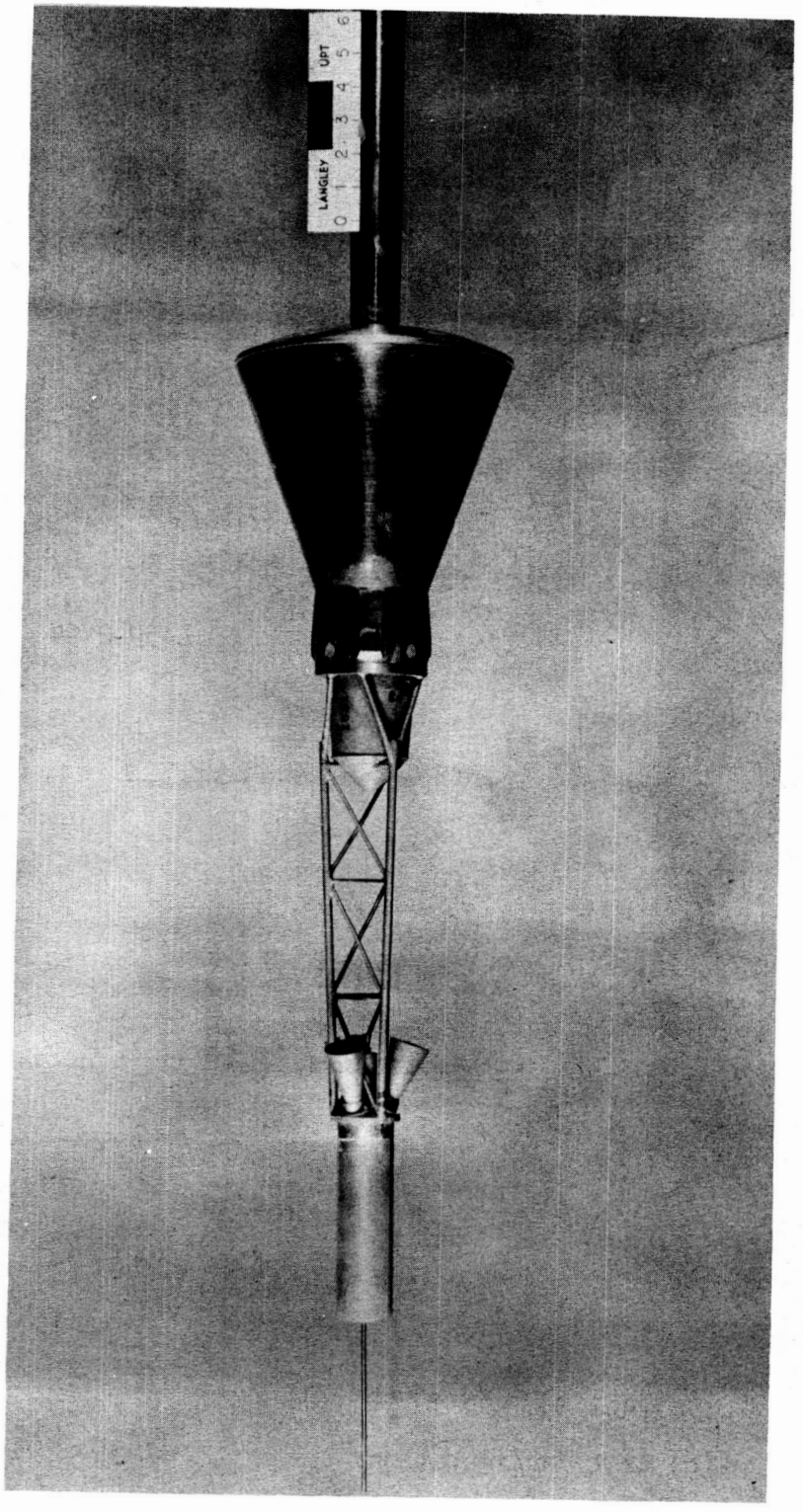

$\alpha = -4^\circ$ to 28°

(a) Escape configuration. L-59-2800

Figure 3.- Sting support arrangements.

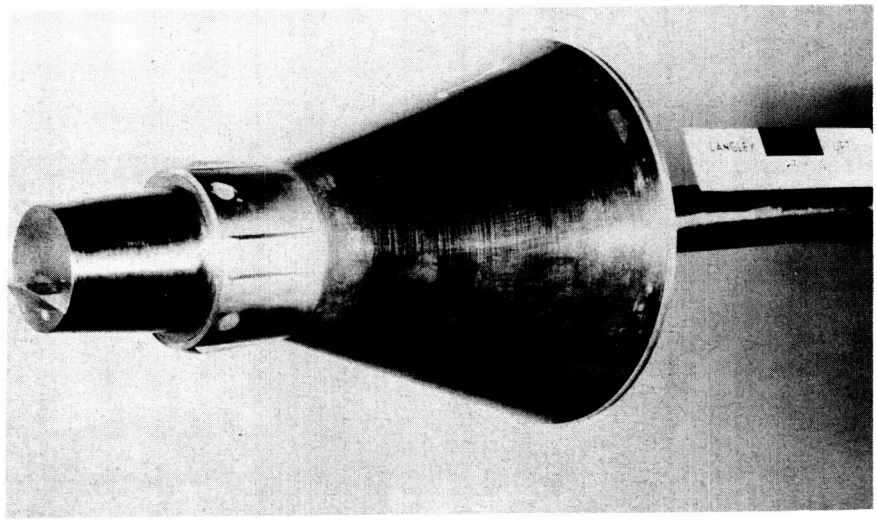

α = -4° to 47°

L-59-2794

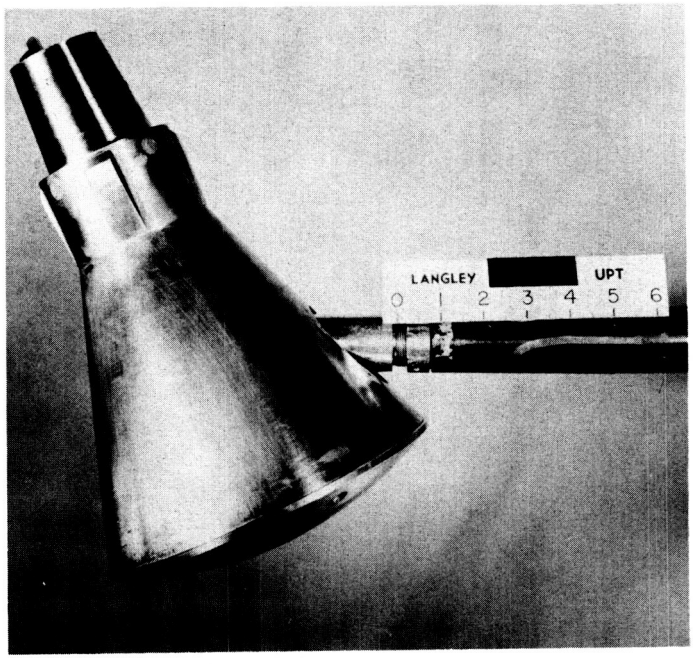

α = 47° to 87°

(b) Exit configuration.

L-59-2793

Figure 3.- Continued.

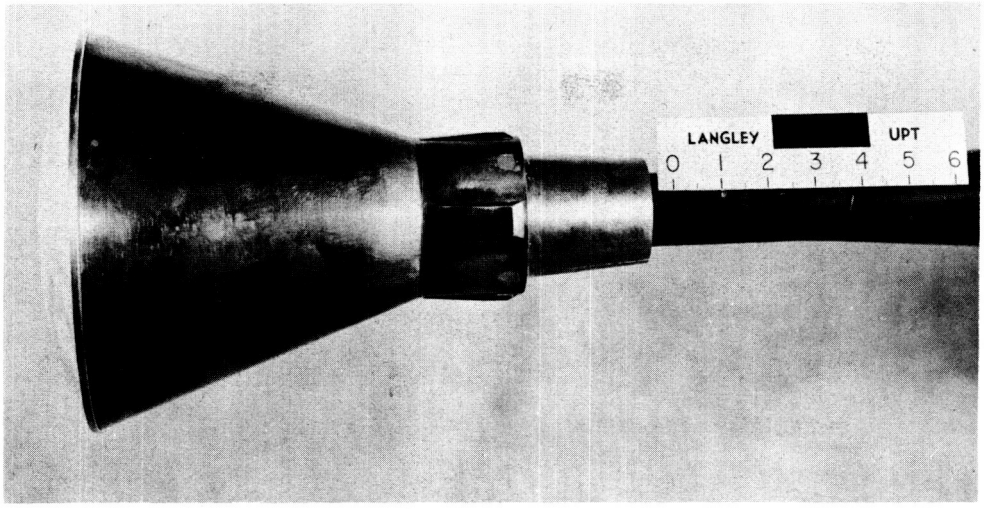

α = -4 to 47°

L-59-2797

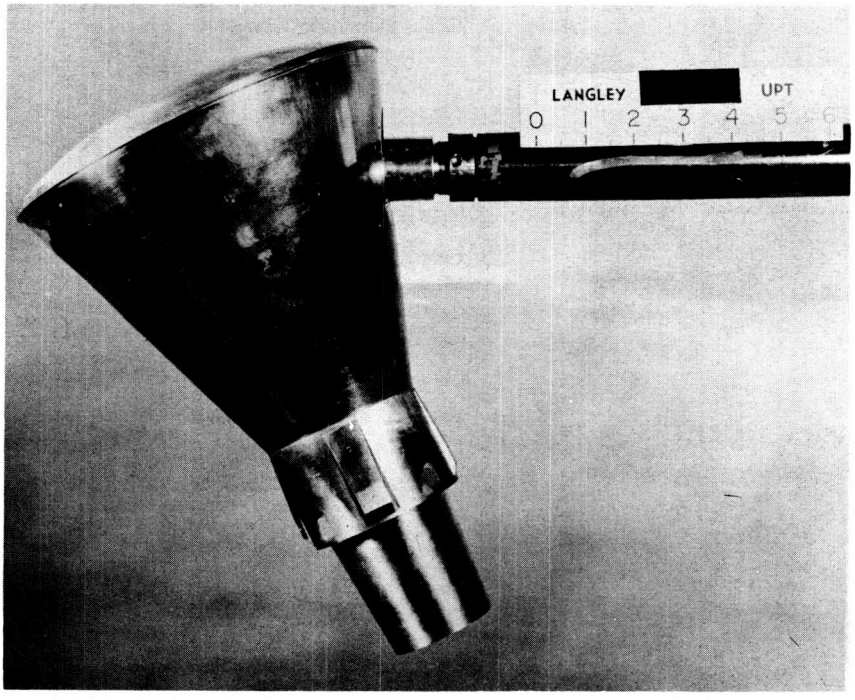

α = 47° to 87°

(c) Reentry configuration. L-59-2795

Figure 3.- Concluded.

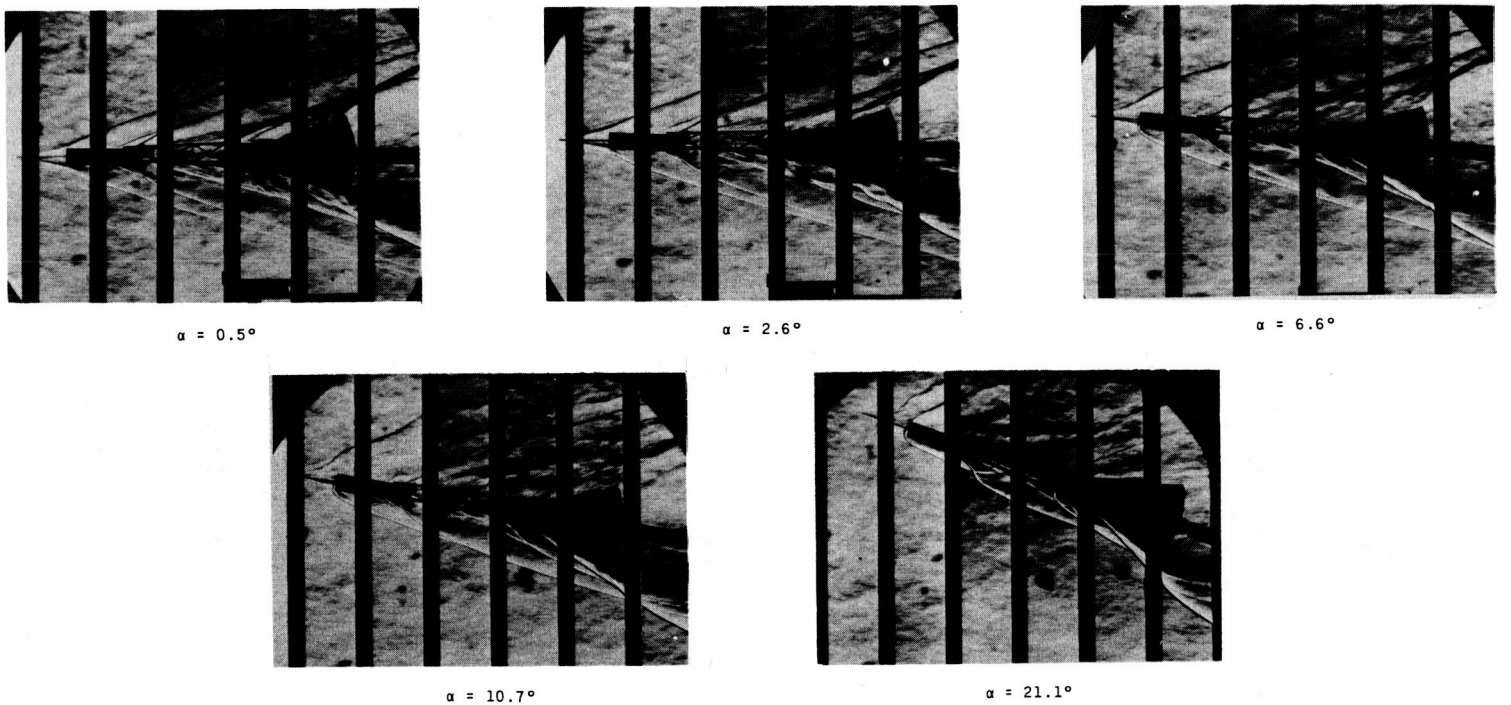

L-60-278

Figure 4.- Typical schlieren photographs of the escape configuration. M = 3.94; R = 2.90 × 10^6.

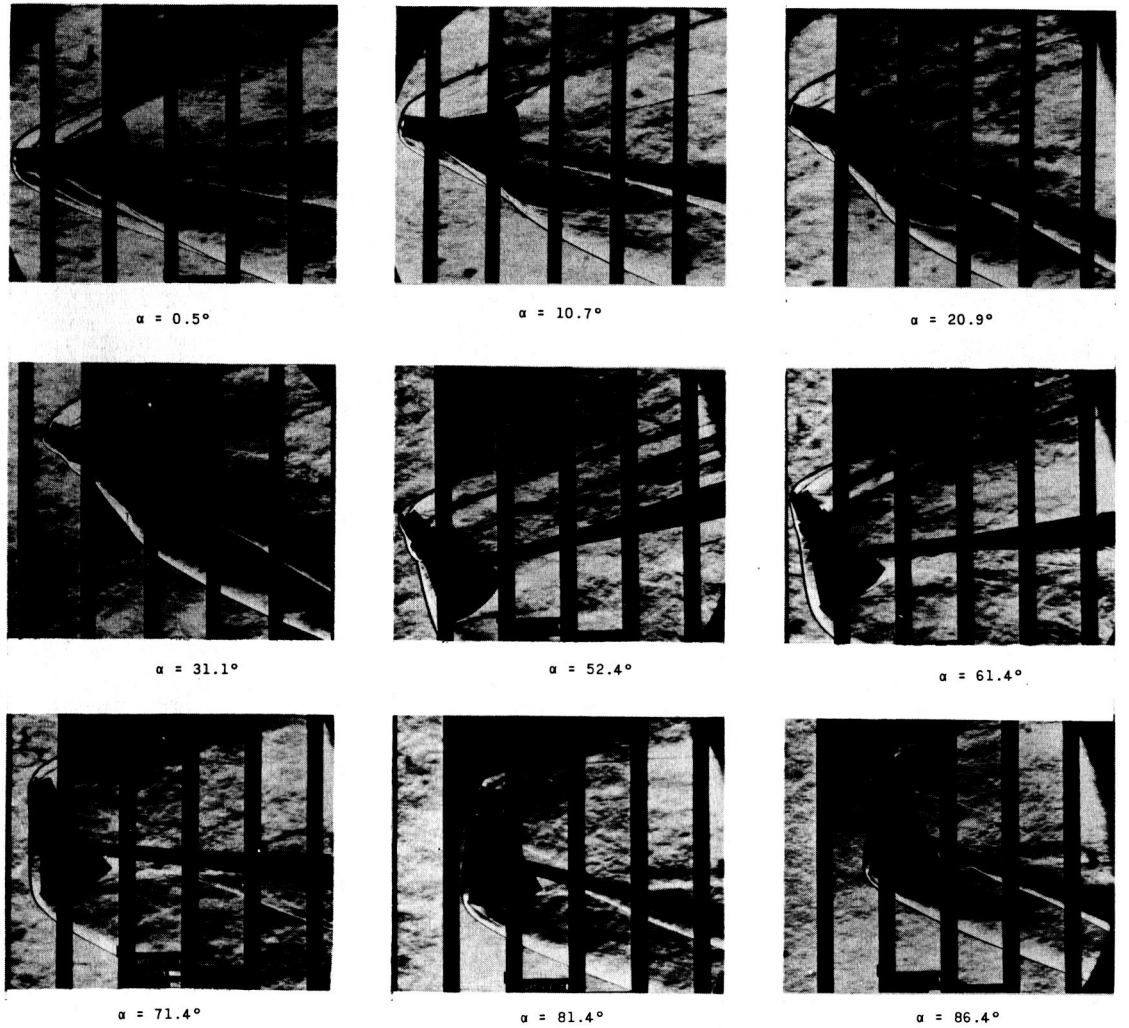

L-60-279

Figure 5.- Typical schlieren photographs of the exit configuration. M = 3.94; R = 2.90×10^6.

CONFIDENTIAL

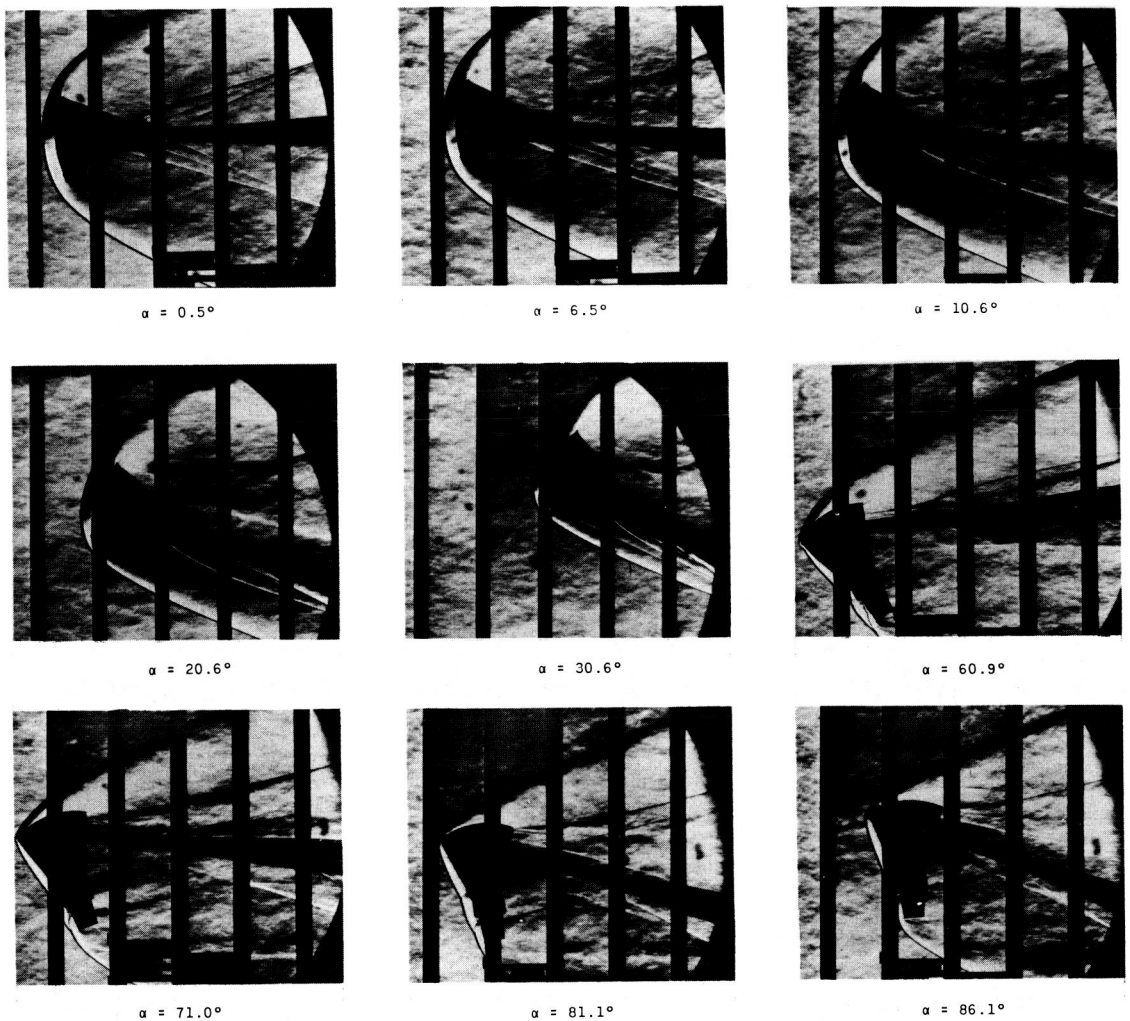

L-60-280

Figure 6.- Typical schlieren photographs of the reentry configuration. M = 3.94; R = 2.90 × 10^6.

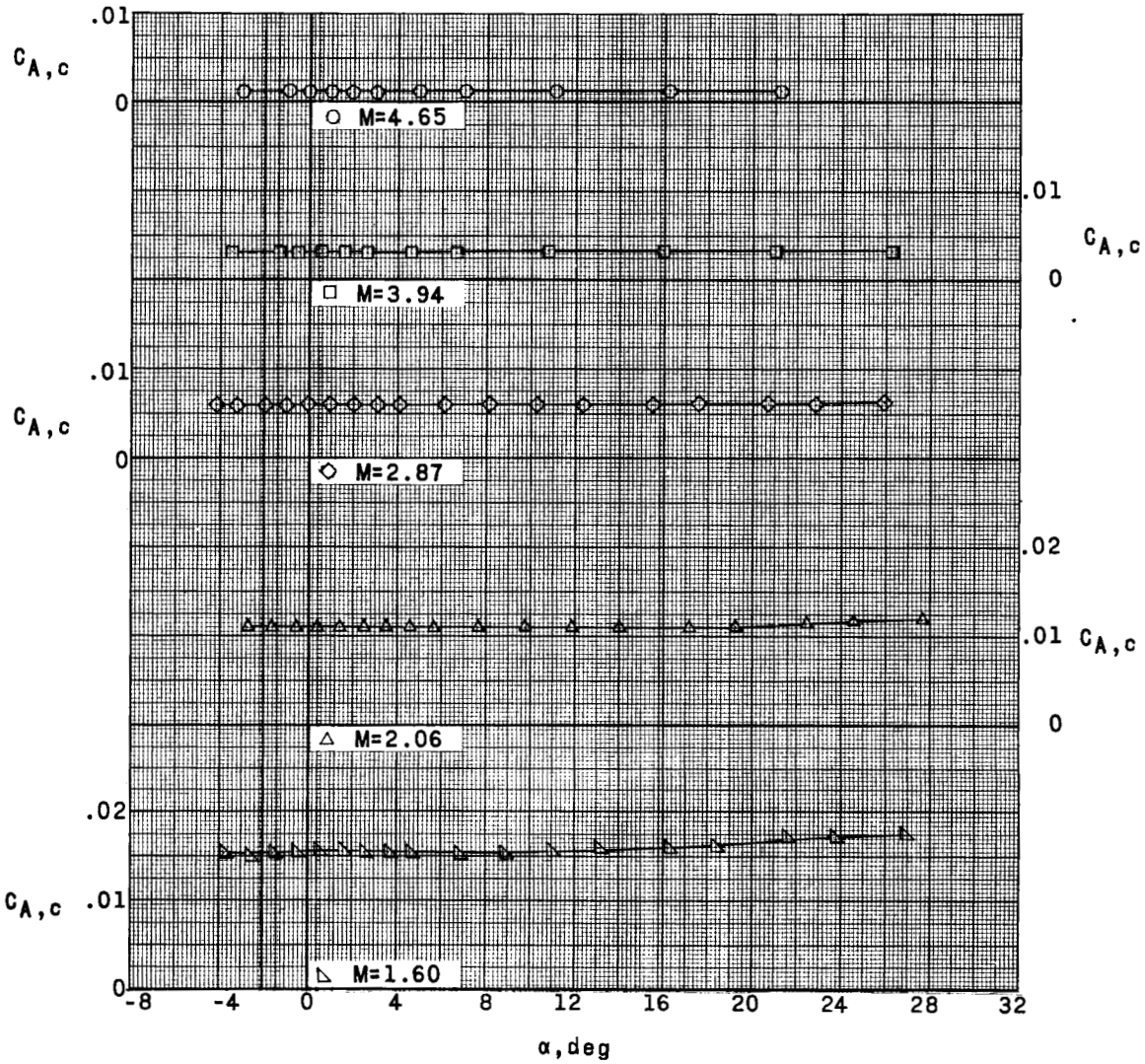

Figure 7.- Chamber axial-force coefficients of escape configuration.

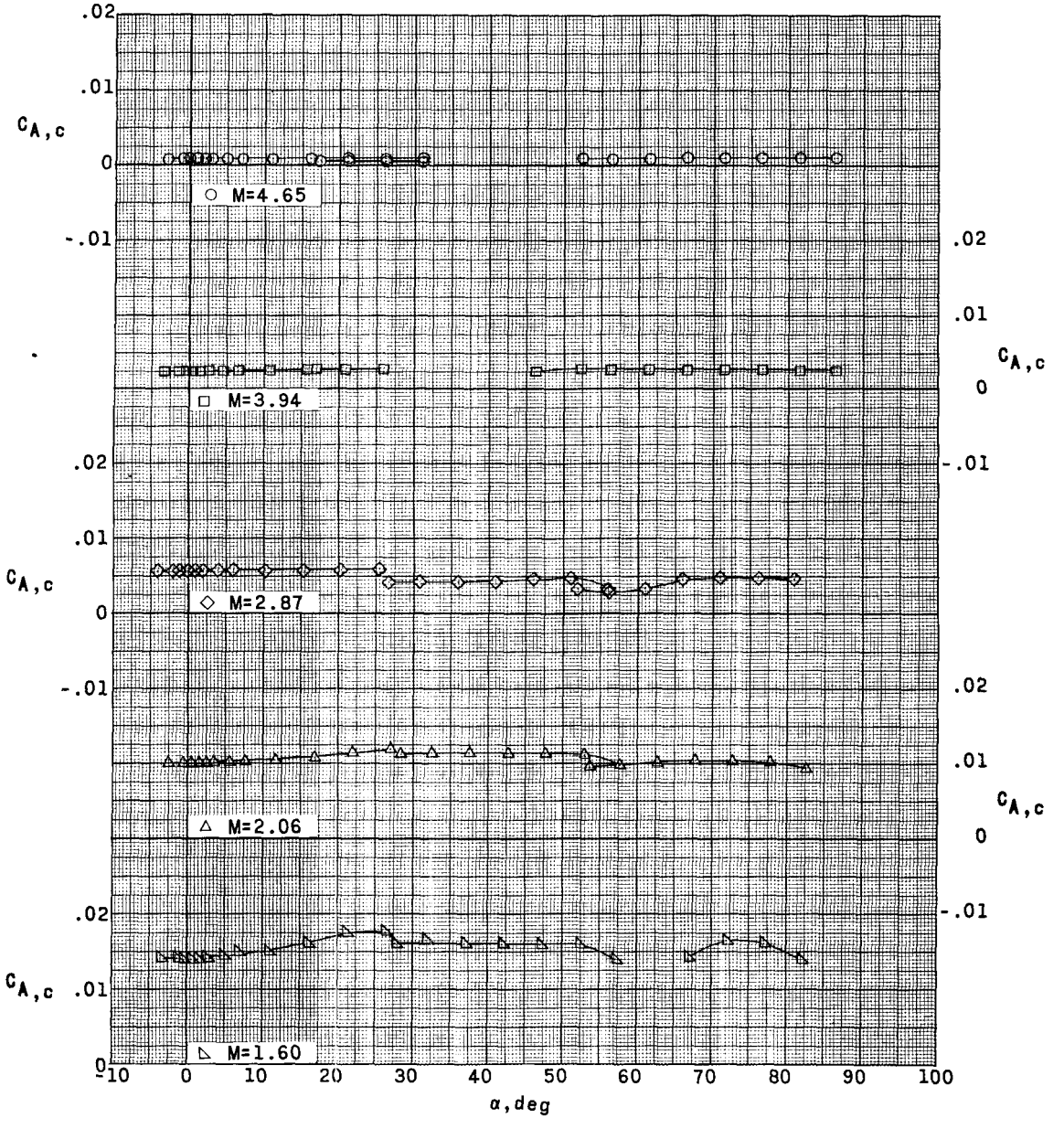

Figure 8.- Chamber axial-force coefficients of the exit configuration.

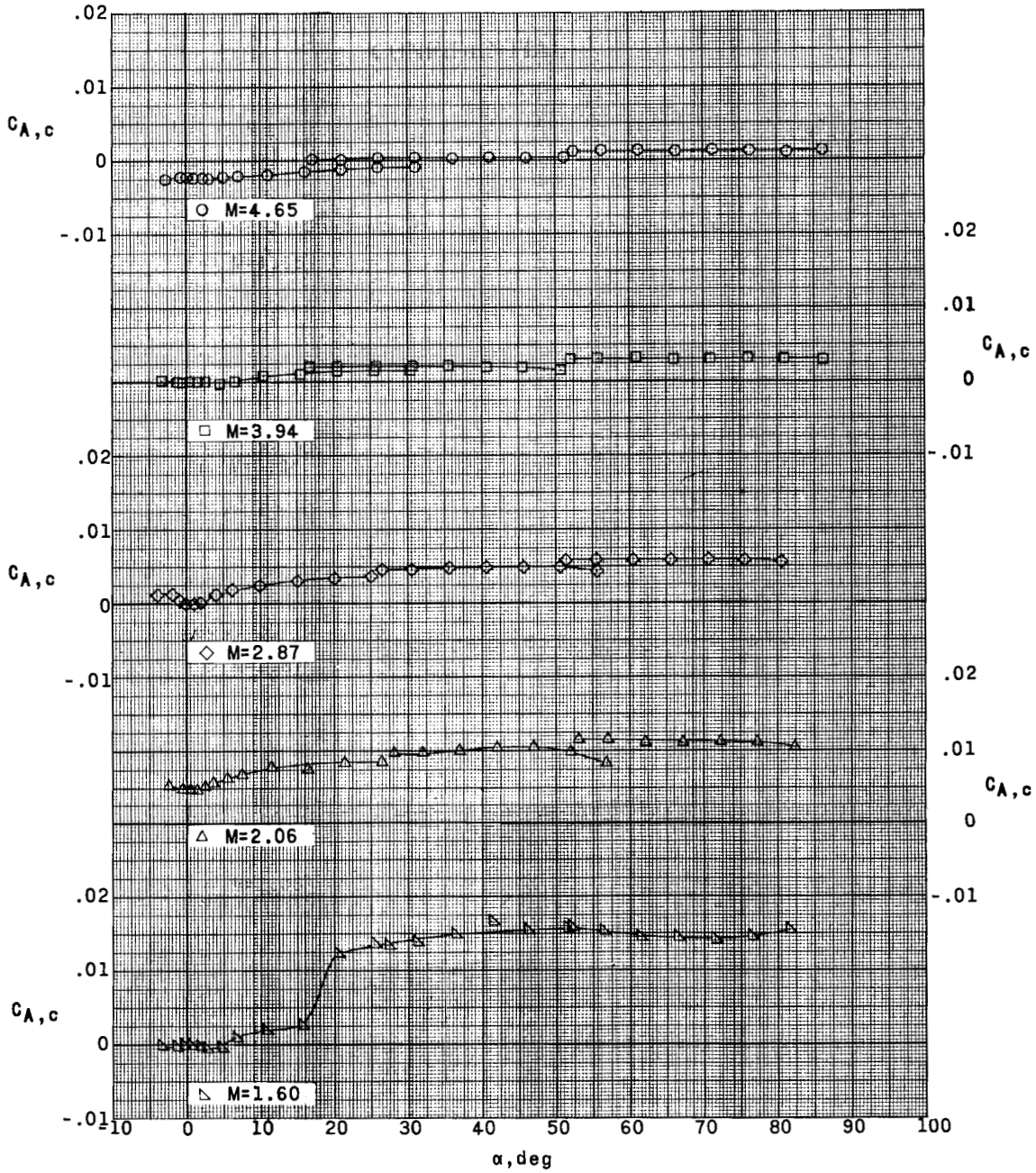

Figure 9.- Chamber axial-force coefficients of the reentry configuration.

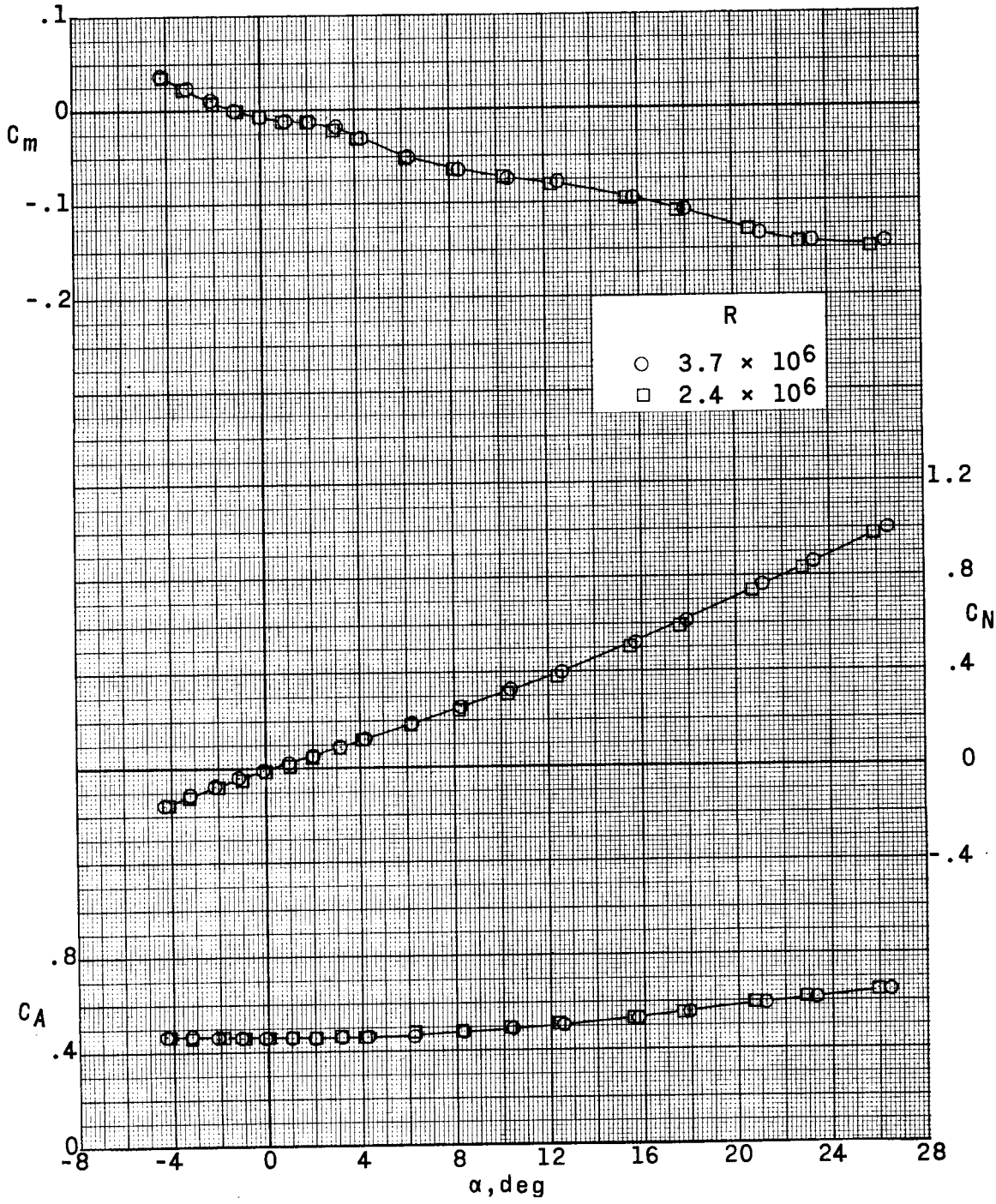

Figure 10.- Effect of change in Reynolds number on the aerodynamic characteristics of the escape configuration. M = 2.87.

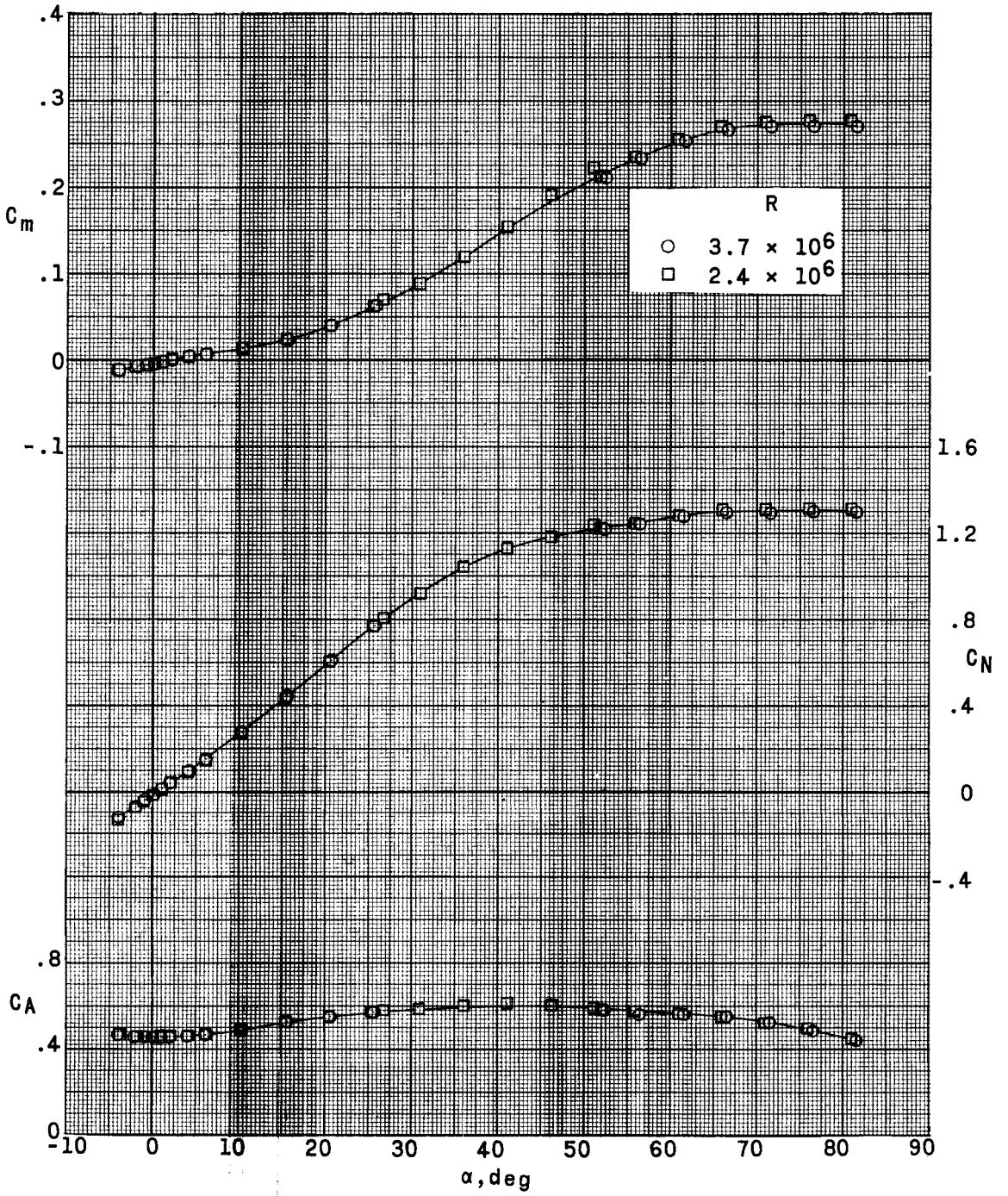

Figure 11.- Effect of change in Reynolds number on the aerodynamic characteristics of the exit configuration. M = 2.87.

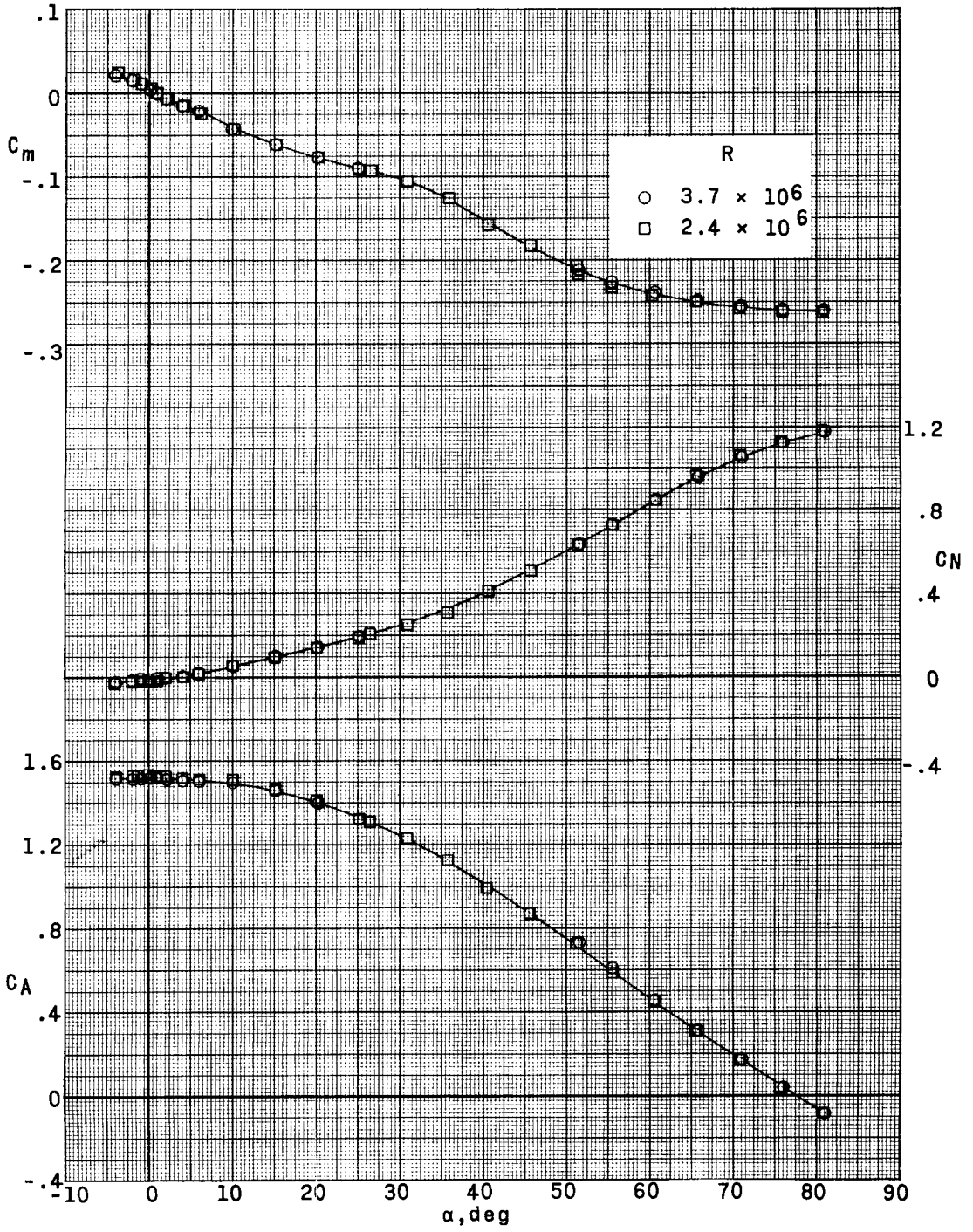

Figure 12.- Effect of change in Reynolds number on the aerodynamic characteristics of the reentry configuration. M = 2.87.

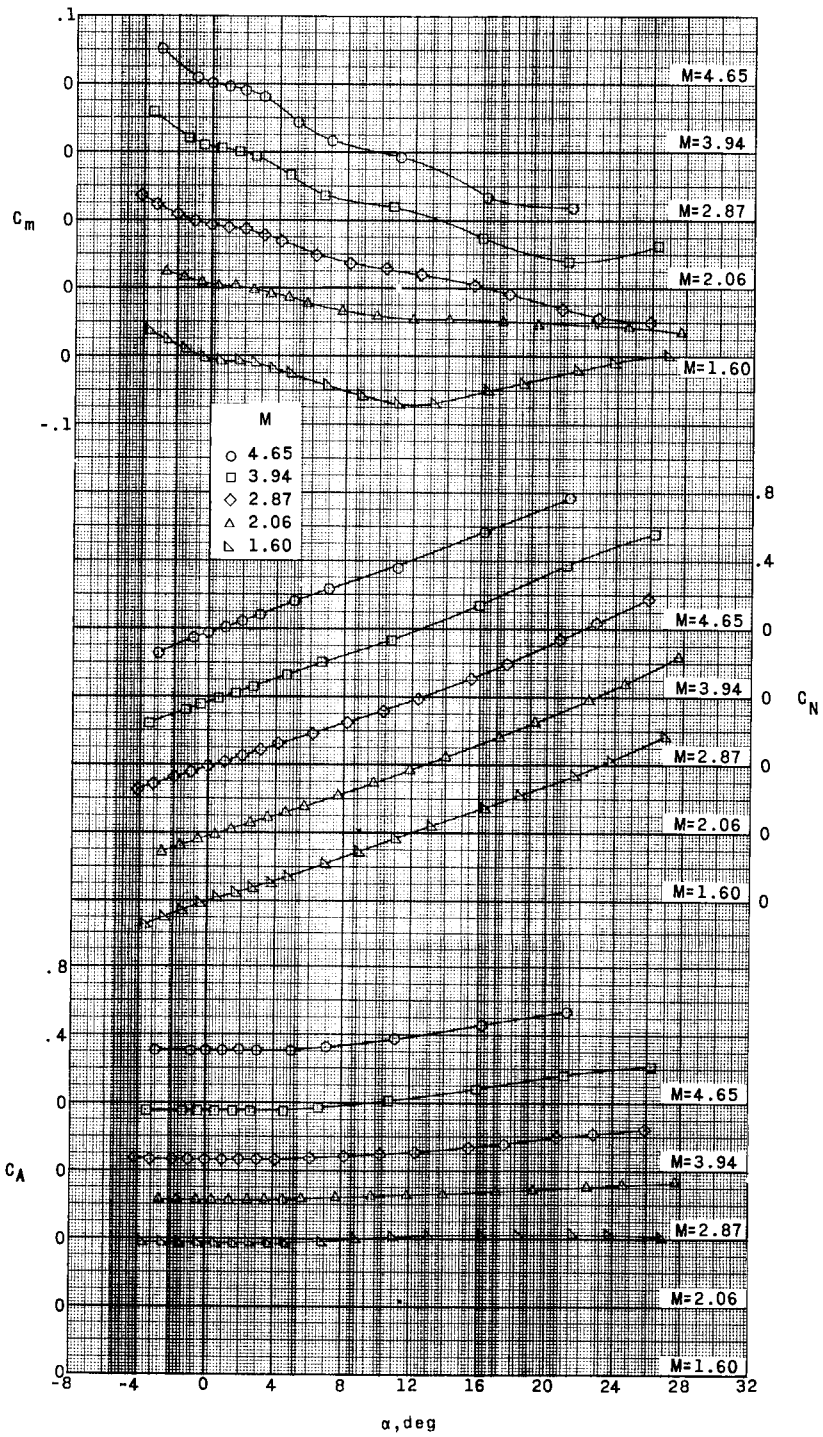

Figure 13.- Aerodynamic characteristics of the escape configuration.

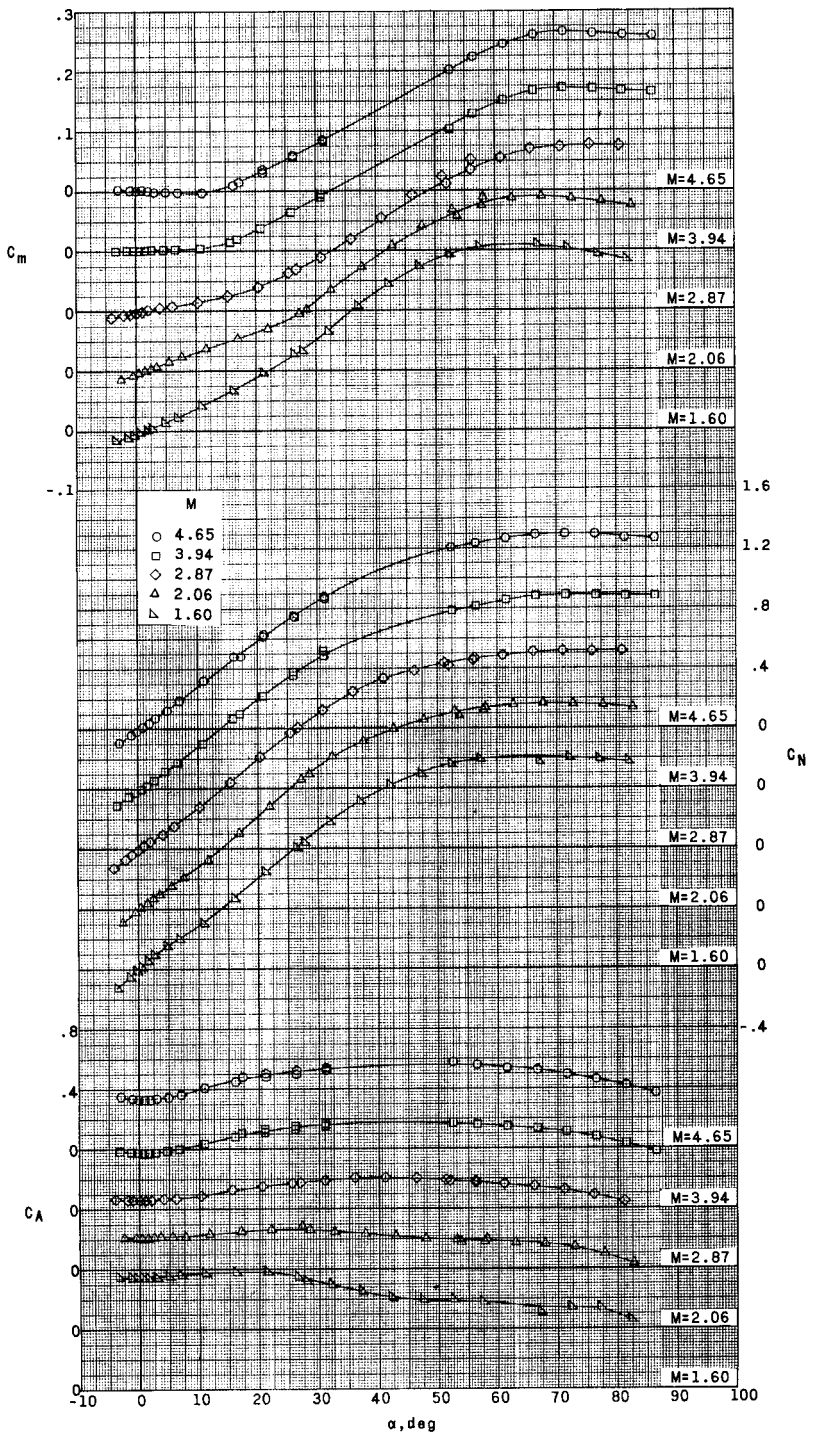

Figure 14.- Aerodynamic characteristics of the exit configuration.

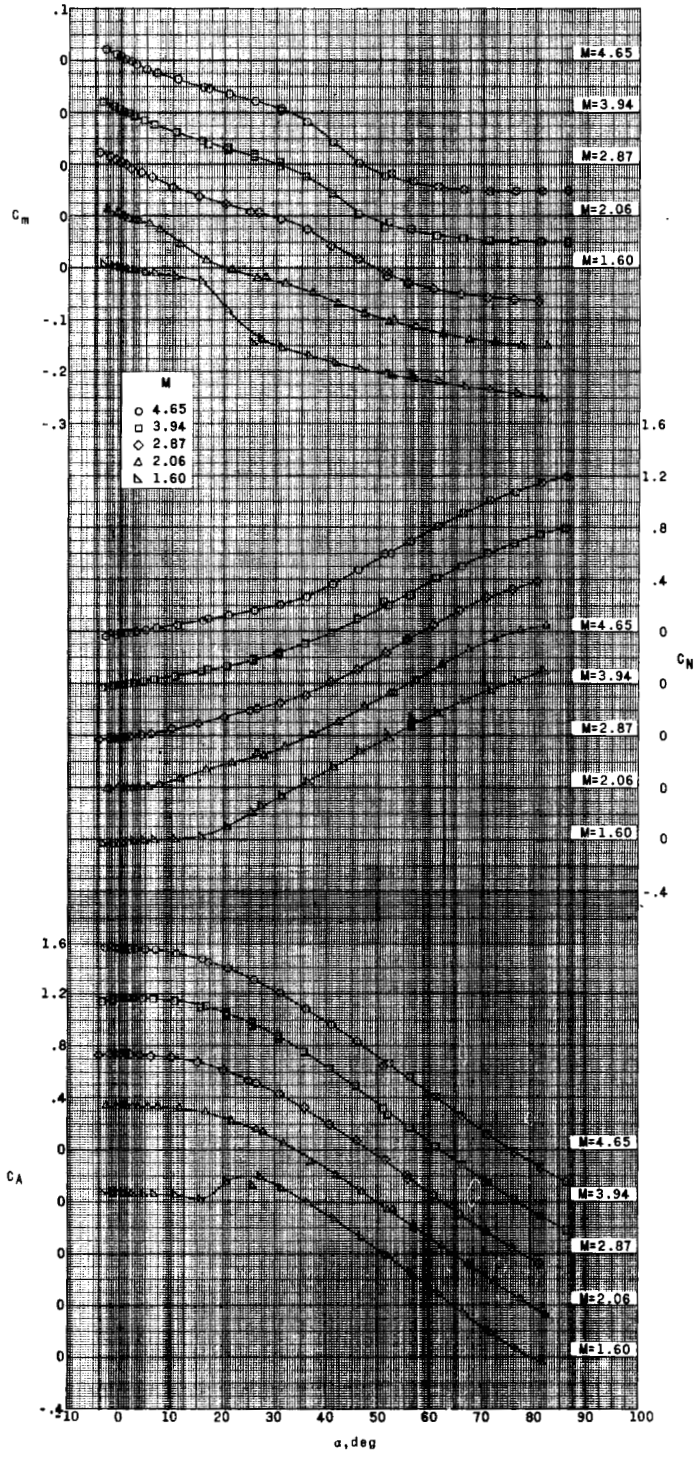

Figure 15.- Aerodynamic characteristics of the reentry configuration.

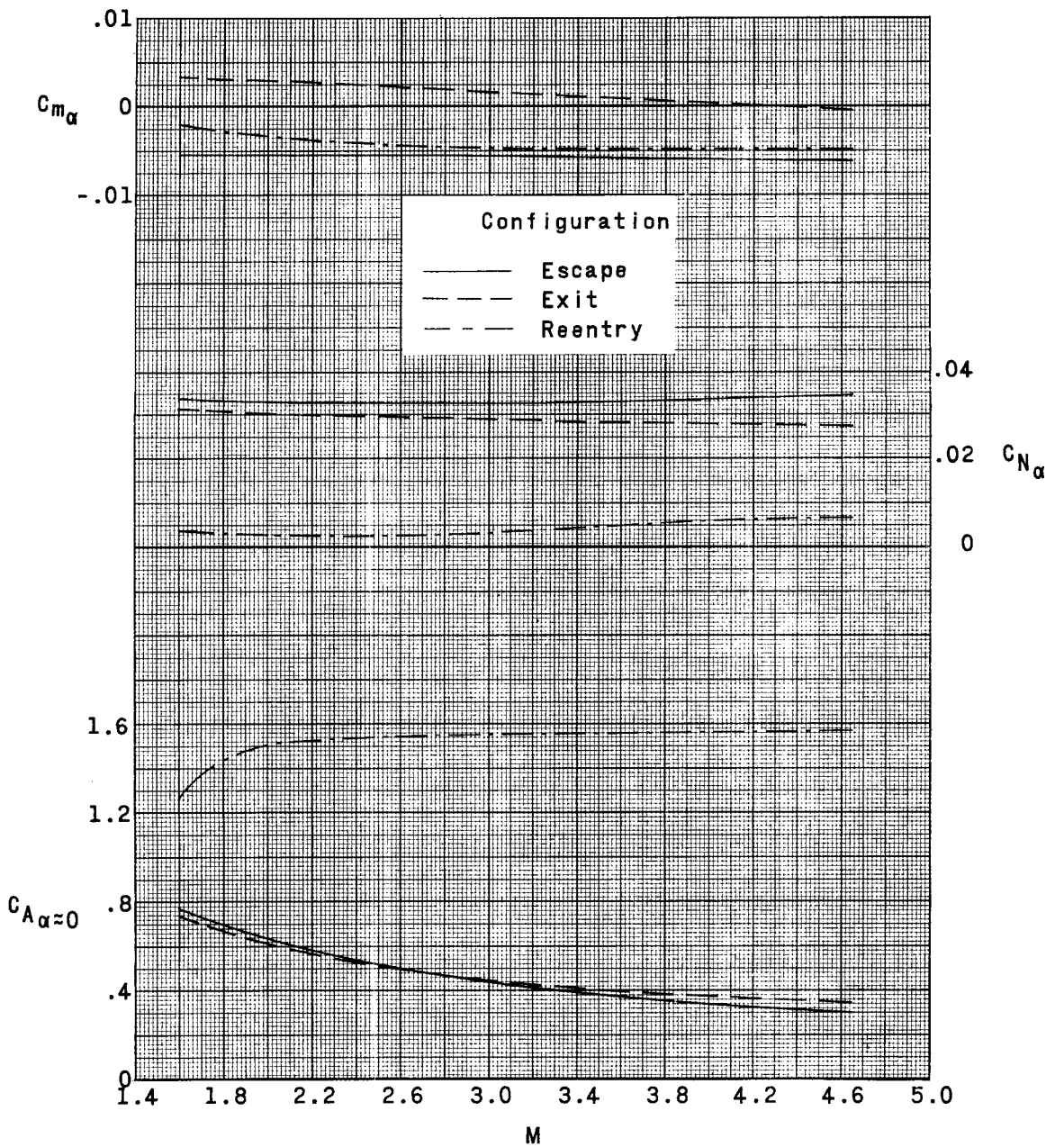

Figure 16.- Summary of stability and axial-force characteristics.